AD-A043 686 SOUTHWEST RESEARCH INST SAN ANTONIO TEX F/G 11/6
CRACK TIP PLASTICITY ASSOCIATED WITH CORROSION ASSISTED FATIGUE--ETC(U)
AUG 77 D L DAVIDSON, J LANKFORD N00014-75-C-1038
UNCLASSIFIED NL

1 OF 1
AD A043686

END
DATE FILMED
9-77
DDC

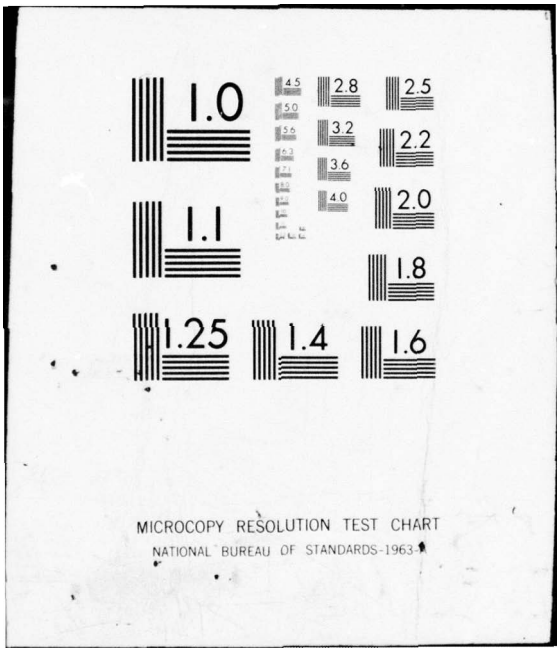
1.0
1.1
1.25
1.4
1.6
1.8
2.0
2.2
2.5
2.8
3.2
3.6
4.0
4.5
5.0
5.6
MICROCOPY RESOLUTION TEST CHART
NATIONAL BUREAU OF STANDARDS-1963-A

(12)

Contract N00014-75-C-1038

CRACK TIP PLASTICITY ASSOCIATED WITH CORROSION ASSISTED FATIGUE

D. L. Davidson and J. Lankford
Southwest Research Institute
P. O. Drawer 28510
San Antonio, Texas 78284

Interim Report for Period June 1976 - June 1977

Prepared for
OFFICE OF NAVAL RESEARCH
800 North Quincy Street
Arlington, Virginia 22217

8 August 1977

UNCLASSIFIED

SECURITY CLASSIFICATION OF THIS PAGE (When Data Entered)

REPORT DOCUMENTATION PAGE

READ INSTRUCTIONS BEFORE COMPLETING FORM

1. REPORT NUMBER

2. GOVT ACCESSION NO.

3. RECIPIENT'S CATALOG NUMBER

4. TITLE (and Subtitle)

CRACK TIP PLASTICITY ASSOCIATED WITH CORROSION ASSISTED FATIGUE.

5. TYPE OF REPORT & PERIOD COVERED

Interim Report.
June 1976 - June 1977.

6. PERFORMING ORG. REPORT NUMBER

02-4268

7. AUTHOR(s)

D. L. Davidson
J. Lankford

8. CONTRACT OR GRANT NUMBER(s)

N00014-75-C-1038

9. PERFORMING ORGANIZATION NAME AND ADDRESS

Southwest Research Institute
P. O. Drawer 28510
San Antonio, Texas 78284

10. PROGRAM ELEMENT, PROJECT, TASK AREA & WORK UNIT NUMBERS

NR 036-109/2-25-76(471)

11. CONTROLLING OFFICE NAME AND ADDRESS

Office of Naval Research
800 North Quincy Street
Arlington, Virginia 22217

12. REPORT DATE

8 August 1977

13. NUMBER OF PAGES

27 plus prelims

14. MONITORING AGENCY NAME & ADDRESS (if different from Controlling Office)

32p.

15. SECURITY CLASS. (of this report)

Unclassified

15a. DECLASSIFICATION/DOWNGRADING SCHEDULE

16. DISTRIBUTION STATEMENT (of this Report)

Reproduction in whole or in part is permitted for any purpose of the United States Government. Distribution is unlimited.

DISTRIBUTION STATEMENT A
Approved for public release;
Distribution Unlimited

17. DISTRIBUTION STATEMENT (of the abstract entered in Block 20, if different from Report)

DDC
RECEIVED
SEP 1 1977
B

18. SUPPLEMENTARY NOTES

19. KEY WORDS (Continue on reverse side if necessary and identify by block number)

Corrosion Fatigue	Low carbon steel
Crack tip plasticity	Electron channeling
Fatigue-environment interaction	Fatigue crack propagation
Crack tip replication	Dislocation subcells

20. ABSTRACT (Continue on reverse side if necessary and identify by block number)

The plasticity associated with propagation of a fatigue crack was found to be altered by a moist air environment, as compared to a dry nitrogen environment. Subcell size distribution and size of the plastic zone are the parameters altered, with the moist air causing a smaller plastic zone with the resulting redistribution of subcell sizes. The energy for crack propagation has been determined by the combination of subcell size and work per cycle required to give that subcell size. This calculation indicates a decrease of 67% in the energy for crack propagation is caused by the moist environment. The moist air environment also

DD FORM 1 JAN 73 1473 EDITION OF 1 NOV 65 IS OBSOLETE

Unclassified
SECURITY CLASSIFICATION OF THIS PAGE (When Data Entered)

328 200

20. Abstract (continued)

alters fracture surface features in a manner consistent with the plasticity results. Hydrogen is believed to be responsible for these changes, in that it can (1) make dislocation motion more difficult, and (2) decrease the strain to fracture. An effort was made to directly detect hydrogen by ion microprobe, but the results were inconclusive.

SUMMARY AND CONCLUSIONS

1. For Fe -.05 wt.%C, a moist air environment (50-70%R.H.) decreases the size of the inner cyclic plastic zone, and alters the subcell size distribution within the plastic zone, as compared to a dry (1 ppm in nitrogen) environment.

2. The energy dissipated within the inner cyclic plastic zone to create a unit area of crack surface is approximately 4.33×10^4 J/m^2 for the dry nitrogen environment and 1.92×10^4 J/m^2 for the moist air environment at $\Delta K = 10$ MN/m$^{3/2}$ (near the threshold of approximately $\Delta K = 6.6$ MN/m$^{3/2}$). This energy calculation is derived from subcell size measurements made using channeling contrast, and from work per cycle data derived from the literature. If correct, this indicates that the energy equivalent value of the moist environment is 2.91×10^4 J/m^2 or 67% of the energy required for crack propagation in the dry environment.

3. Observation of the crack profiles, and fractography of the fracture surface indicate a marked decrease in plasticity associated with the moist environment.

4. All of the above data point to hydrogen as the active specie in the moist air which is responsible for these effects. Hydrogen is believed to have two effects: 1) increase the flow stress of the affected material and 2) decrease the deformation before fracture. An increase in flow stress is supported from data found in the literature, and the decrease in deformation to fracture is supported by our experimental findings.

5. An effort to obtain direct evidence for hydrogen was made by Dr. Dale Newbury at NBS using an ion microprobe. The data, although interesting, are inconclusive.

TABLE OF CONTENTS

INTRODUCTION

This annual report includes a brief description of the first year of work, for continuity, then reports on the results of the second year for Contract N00014-75-C-1038, entitled "A Study of the Crack Tip Plasticity Associated with Corrosion Assisted Fatigue."

Last year, the discovery was made in Fe -.05 wt.%C that the subcell size distribution created by passage of a fatigue crack is altered by the water vapor content of the gaseous environment in which the crack was propagated. This discovery was made using electron channeling contrast in the scanning electron microscope.

This year, the influence of cyclic stress intensity on subcell size, as coupled with the water vapor effect, and a determination of the energy of crack propagation, have been the principal topics of study. Some further study of the channeling contrast technique itself was also completed.

I. THE INFLUENCE OF WATER VAPOR ON FATIGUE CRACK PLASTICITY IN Fe - .05 wt.% C

A. Quantifying The Effect

Last year, it was clearly shown that water vapor influences the subcell size caused by a propagating fatigue crack in low carbon steel.[1,2] Subsequent testing has shown that while this observation is correct, it is difficult to quantify with a high degree of confidence. The reasons for this difficulty are not entirely understood; however, one of the major sources of statistical variation is sure to be the response of a randomly oriented polycrystalline aggregate to the non-linear stress gradients in the vicinity of a crack tip. Furthermore, high magnification photographs (1000x) are required to reveal the detail of substructure necessary for analysis. Such photographs are not difficult to make, but their analysis is time consuming, and since each photograph covers only a small number of grains, a large number of them must be analyzed to obtain statistically meaningful values.

Data from cracks propagated in dry nitrogen (1 ppmv as measured by a dew point indicator 1 cm from the crack) at only one value of ΔK (cyclic stress intensity) yield reproducible results, which are shown in Figure 1(a). Data from cracks propagated in air at ambient humidity, generally 50-70% do not show such consistency, as is illustrated for 3 specimens in Figure 1(b). The variation in the slope of the ambient humidity air data are similar, but less pronounced, than the variation caused by changing ΔK, Figure 1(c). At larger values of ΔK, the variation in subcell size distribution caused by interaction with the environment decreases, Figure 1(d).

For both environments and all ΔK investigated, subgrain size (d) is a linear function of distance (r) from the crack plane. Where the subgrain size approaches the mean grain size, there is a short transition region. Thus, $d = A + Br$ describes the subgrain size out to a distance r_1 (where the subgrain size equals the average grain size) better than other functional dependencies with only small inaccuracy. Table I contains the best values of the constants obtained to date.

The specimen which has been used thus far is of the center notch design, with alternating wet and dry environments used for each specimen at several levels of ΔK. Crack propagation rates have been measured as total change in crack length per cycle, which indicates very little difference between dry nitrogen and ambient humidity, with $\frac{da}{dn} \text{ Const } (\Delta K)^{3.80}$. This compares with an exponent at 3.73 as measured by Yokobori, et al[3] for the same material, and with values between 2.8 and 3.6 as measured from data on 1020 steel from Nelson.[4,5] In order to obtain more accurate crack growth data, single edge notch specimens are now being used, each specimen in a single environment with an ever increasing ΔK. "Ambient" humidity will also be controlled to a constant value.

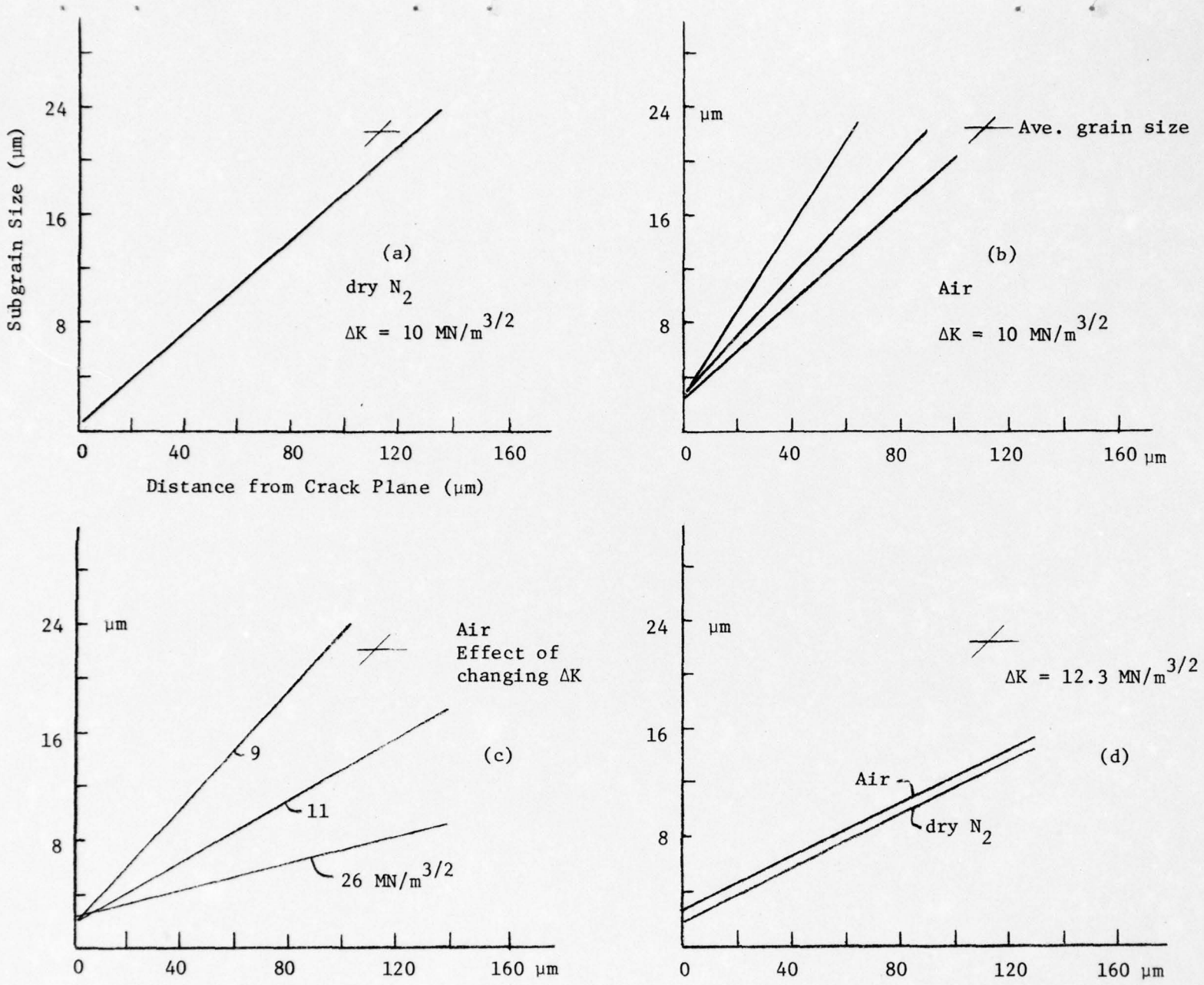
Subgrain Size (μm)
24
16
8
0
40
80
120
160
Distance from Crack Plane (μm)
(a)
dry N_2
ΔK = 10 MN/$m^{3/2}$
μm
Ave. grain size
(b)
Air
ΔK = 10 MN/$m^{3/2}$
Air
Effect of
changing ΔK
9
11
26 MN/$m^{3/2}$
(c)
ΔK = 12.3 MN/$m^{3/2}$
Air
dry N_2
(d)

FIGURE 1

Table I.

Envn	ΔK ($MN/m^{3/2}$)	$\frac{da}{dn}$ 10^{-10} m/c	A (μm)	B ($\mu m/\mu m$)	r_1 (μm)
Wet Air (12,000 ppmv)	7.5	5.1	2.45	.233	85
	8.8	22	6.45	.144	108
	8.8	22	4.73	.186	93
	9.4	16.5	2.24	.254	78
	9.4	16.5	0.88	.368	60
	10.5	34	3.47	.150	125
	10.5	22.5	1.3	.237	88
	10.5	34	3.0	.170	113
	12.3	63.2	1.5	.10	170
Dry N_2 (1 ppmv)	8.7	15.5	0.8	.198	107
	9.8	23.4	0.25	.176	125
	10.5	19.4	1.53	.116	140
	10.5	19.4	1.6	.134	150
	10.5	22.5	1.3	.237	88
	12.3	30.7	0.74	.123	.142

B. Energy for Crack Propagation*

The energy expended in the material by passage of the propagating crack may be calculated from the distribution of subcell sites left in the wake of the crack, Table I, together with other information. The methodology used for the calculation is shown in Figure 2. The work per cycle is taken from the data of F. V. Lawrence and R. C. Jones[6] who studied the formation of subcells in iron single crystals subjected to reverse bending cycling. They operated at stresses betweeen ± 124 and ± 207 N/mm^2, which gave saturation strains of 2.7×10^{-4} to 1.65×10^{-3}. Subcell size was measured by etch pitting, both as a function of number of cycles and cyclic stress. Mughrabi, et al[7] have published hysteresis loops for pure iron, which indicate that the total energy per cycle may be calculated within a few percent (~ 3%) accuracy by multiplying the stress range by the plastic strain range. Strain rate effects are important for iron,[7] but

*An expanded and more complete version of this section will be presented at the symposium "Environment Sensitive Fracture of Engineering Materials" sponsored by AIME, Chicago Oct. 24-27, 1977, and will be submitted for publication in the proceedings of the symposium.

CALCULATION OF ENERGY OF CRACK PROPAGATION

a = crack length

r = distance from crack plane

d = subgrain size

r_1 = extent of plasticity

W_C = work per cycle done on an element

dr x da per unit volume J/m^3

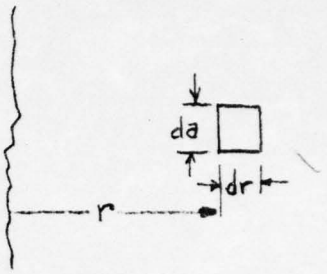

crack plane

W_{CR} = work per cycle done on an element of width da by passage of the crack per unit area of crack

$$= \sum_{0}^{r_1} W_C \qquad J/m^2$$

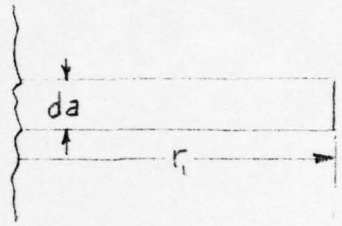

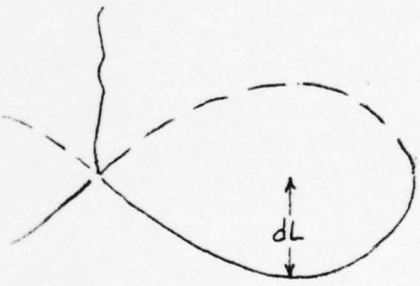

$N(r)$ = the number of cycles influencing an element da

$$= \frac{dL}{da/dn}$$

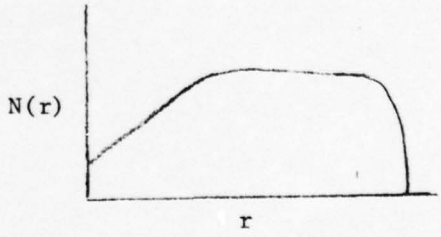

W_T = total energy expended due to crack passage per unit area of crack

$$= 2 \sum_{0}^{r_1} \sum_{0}^{N} W_C(r)\, N(r)$$

$W_C = 2.97\, d^{-1.097}$ $\qquad d = A + Br$ $\qquad$ determine dL graphically

From Lawrence and Jones,
Met. Trans. 1 367 (1970)

FIGURE 2

have been neglected in these calculations as a second order effect. The relationship between work per cycle and bulk subgrain size resulting from analysis of Lawrence and Jones' data is shown in Figure 3. The line drawn through the data is $W_c = 2.97\ d^{-1.097}$. Sensitivity of the magnitude of the calculated energy to the slope of this line will be discussed later.

Referring again to Figure 2, determination of the number of cycles N(r) influencing an element was determined by looking at several sections of several crack tips all propagated at the same ΔK. A typical section is shown in Figure 4; the two sets of photographs are identical, but with the lower set having an overlay showing the calculated plain strain cyclic plastic zone. By looking at this and six other similar sections, we have determined that the crack influence begins at about the leading edge of this zone and has reached equilibrium at about the center line of the zone. Figure 4 is shown for dry nitrogen, but the situation is similar for the wet environment, while less well documented at this time. From data such as Figure 4, dL(r) can be determined graphically, and by dividing by da/dn, then N(r) is determined.

Calculation of the total energy for crack passage is the sum of the work per cycle multiplied by the number of cycles for each element within the influence of the crack, adjusted to a unit area of crack surface area.

We have shown previously[3] that subgrains are forming in the inner cyclic zone of the total plastic zone formed by the crack. The work calculation thus does not include the outer monotonic plastic zone.

So far, the energy for crack propagation calculation has only been carried out for $\Delta K = 10\ MN/m^{3/2}$, because of the difficulty of determining N(r). The following average values of the measured parameters from Table I were chosen for the calculation:

Env.	A	B	r_1	$\frac{da}{dn}(10^{-10}m/c)$
Wet Air	3.23	.16	120	34
Dry N_2	1.55	.125	160	20

For both dry N_2 and humid air, N(r) was taken to be

$N(r) = 10^4 + 10^2 r$ 0 to 40 μm and

$N(r) = 1.4 \times 10^4$ 40 μm to r_1

These values are close to those actually measured in dry nitrogen. N(r) has not yet been measured for the humid air environment. By assuming the same value for wet air, the energy calculated will be slightly too large, but well within the probable error due to the other assumptions.

The total work done by the crack, W_T, is thus

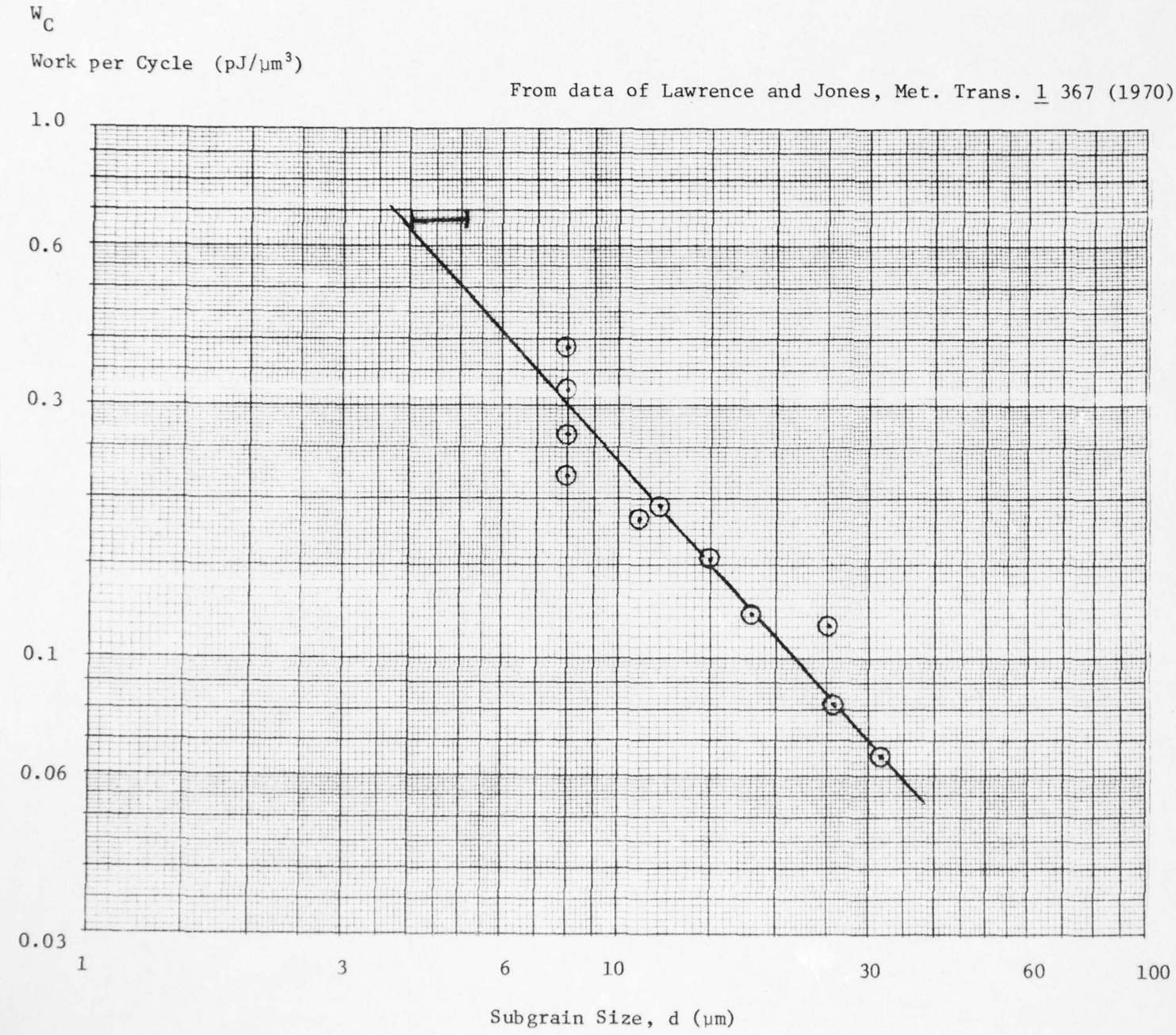
W_C
Work per Cycle (pJ/μm³)
From data of Lawrence and Jones, Met. Trans. 1 367 (1970)
1.0
0.6
0.3
0.1
0.06
0.03
1
3
6
10
30
60
100
Subgrain Size, d (μm)

FIGURE 3

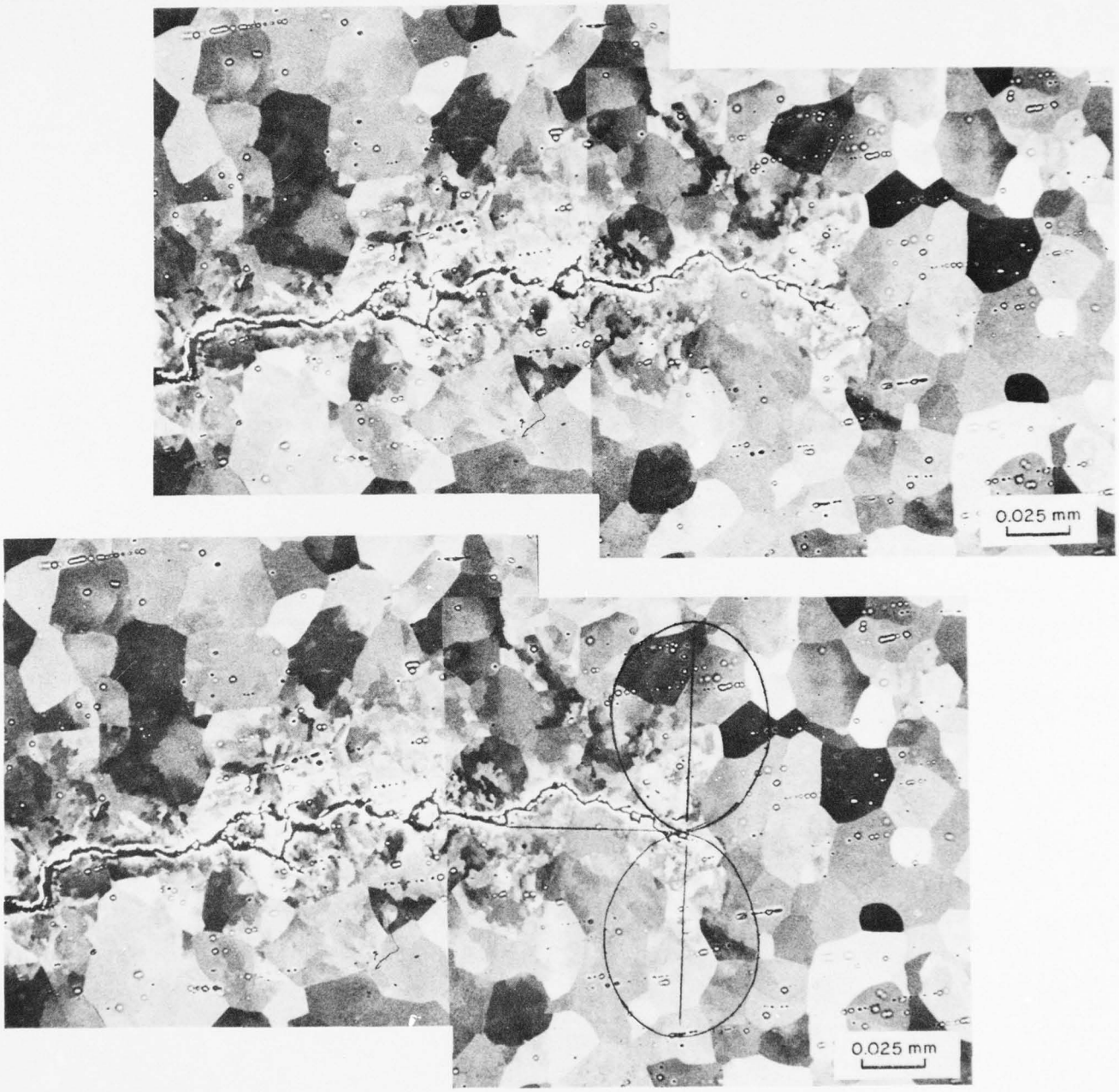

Fe-0.05 C $\Delta K = 9.3\ MN/m^{3/2}$ Dry Nitrogen

Outline shown at crack tip is the calculated plane strain cyclic plastic zone.

FIGURE 4

$$W_T = 2L_1\left[\int_0^{r_1} W_c(r)N(r)dr + \int_{r'}^{r_1} W_c(r)N(r)dr\right]$$

where $L_1 = L(r)$ max = 40 μm for this case, and the other functions were given previously.

Inserting all the numbers and integrating gives the values shown in Table II.

Table II.

Envn.	Energy/Unit Area of Crack Plane(J/m^2)
Dry N_2	4.33×10^4
Wet Air	$\underline{1.42 \times 10^4}$
	2.91×10^4 = energy equivalent of the environment

An analysis of the sensitivity of these values to the magnitude of the experimentally measured factors and to assumptions has been made and will be reported subsequently. Briefly, however, it was determined that values of W_T vary by a factor of 2 for the dry N_2 calculation when the variables are changed by amounts thought to be within reason. The most important assumption is clearly that used for the work per cycle, W_c, which was derived from the data of Lawrence and Jones.[6] This assumption must be checked experimentally.

If the calculation is correct, the environment is supplying the equivalent of 67% of the energy needed for crack propagation in the wet environment. As compared to the energy of crack propagation in dry N_2 of 4.8×10^4 J/m^2, the surface energy of iron is about 2 J/m^2.

Another measurement of the energy of crack propagation (for a high strength, low alloy steel, σ_y = 358 MPa) has been made by Ikeda, Izumi, and Fine.[8,9] For $\Delta K = 9.3$ $MN/m^{3/2}$, $da/dn = 30 \times 10^{-10}$ m/c and the total energy per unit area of crack area was found to be 6×10^5 J/m^2. Since $\frac{da}{dn} = \text{Const.} \frac{(\Delta K)^m}{\mu\sigma^2 u}$, where μ = shear modulus, σ = cyclic yield stress, and U = energy to create a unit of crack surface, we can calculate the approximate value of U for our Fe -.05C material. The constant in the above equation is not well defined, but experimentally[10], it has been determined to be 2.2×10^{-3}. Using this value, $\sigma = 1.2\sigma = 261.6$ MPa, $\mu = 7.8 \times 10^4$ MPa, $m = 3.8$, $\Delta K = 10$ $MN/m^{3/2}$ and $da/dn = 34 \times 10^{-10}$ m/c gives $U = 7.65 \times 10^5$ J/m^2 which is about 10 times larger than the value we determine.

C. Fractography

Scanning electron microscopy of specimens fatigued alternately in humid air (50-70% rh) and in dry nitrogen (1 ppm water vapor) at various stress intensities reveals distinct differences in microfracture mechanisms due to the changes in environment. Portions of the fracture surface created in N_2 are covered in with ductile, transgranular striations. However, regions of the crack plane formed during cycling in moist air have additional features. Some 20% of the surface consists of fracture facets having the appearance of transgranular cleavage. This environmentally-induced fracture mode variation is shown in Figure 5, and in Figure 6a, 6b; it appears that the density of facets is considerably higher in the specimen interior compared to the near-surface region.

Inspection at higher magnification (Figure 6c, 6d) reveals that the facets are not smooth, but are composed of brittle striations. Both brittle and ductile striation spacings exceed the average crack growth per cycle by a factor of approximately 10^2. The size of the brittle-striated facets is roughly equal to the average grain size (23 μm), in accordance with their transgranular appearance.

D. Discussion

The size of the cyclic plastic zone changes both with ΔK and with the environment. The effect of change due to environment is greatest for lower ΔK values, and decreases as ΔK increases. The threshold ΔK for this material is thought to be approximately 6.6 $MN/m^{3/2}$. The maximum change in subcell size due to environment should be, and is, found for ΔK values near and just above threshold because:

1) The difference in slopes of the subcell vs. distance curves are greatest,

2) The energy stored in the plastic zone is minimal, thus allowing the maximum effect of environment to be observed.

A similar effect of environment on plastic zone size has been found in Al-Cu-Mg alloy,[11] where a fatigue crack grown in moist air exhibited a cyclic plastic zone approximately one-half that of a crack grown in vacuum.

To explain this effect, we have concluded, together with other investigators,[12, 13] that hydrogen is the environmental specie responsible. The scant direct evidence of its presence is presented in the next section. Thus, at this time we can only infer that it is hydrogen which is the active specie from indirect measurements and fractography.

Hydrogen can only be influential if it is present, probably in ionic form, either at the surface of the crack tip, or within the lattice near the crack tip. The presence of hydrogen could 1) affect the motion of dislocations within the lattice and 2) affect the fracture characteristics of

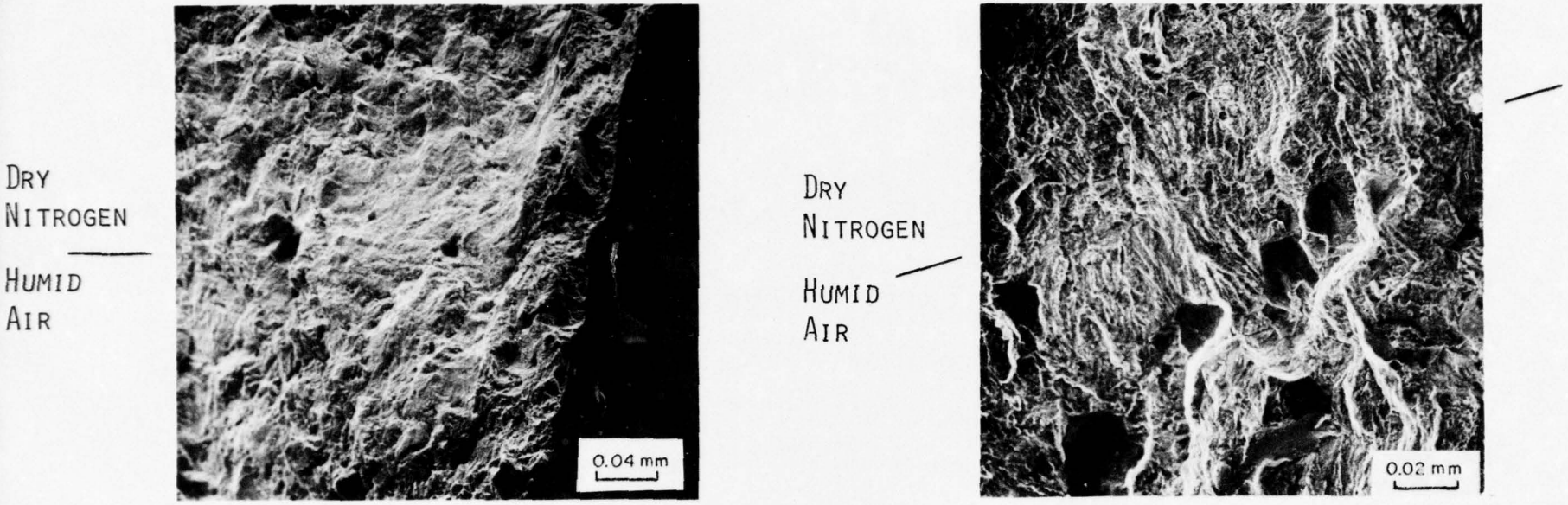

(a) (b)

FE-0.05 C FRACTURE SURFACE SHOWING THE EFFECT OF CHANGE IN ENVIRONMENT.

FIGURE 5

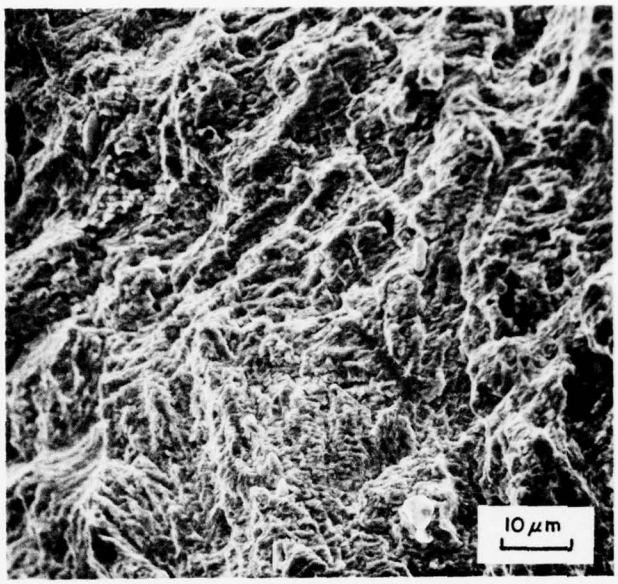

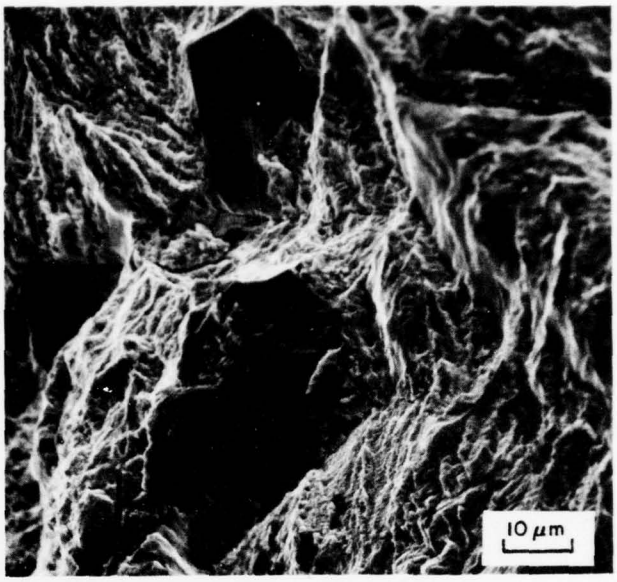

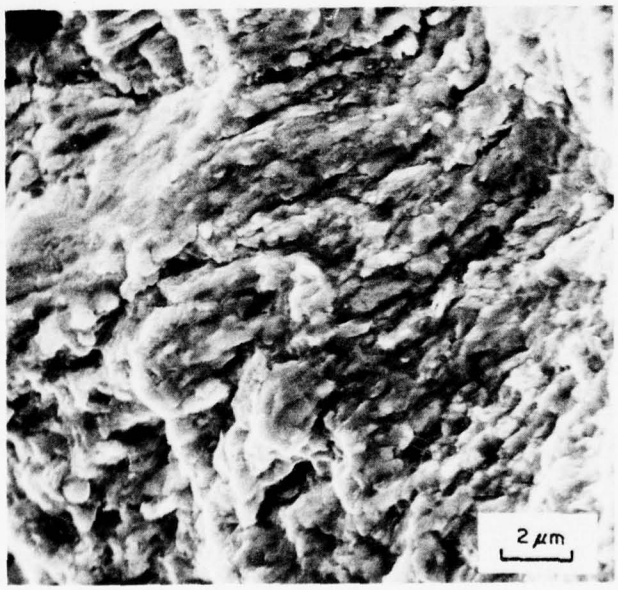

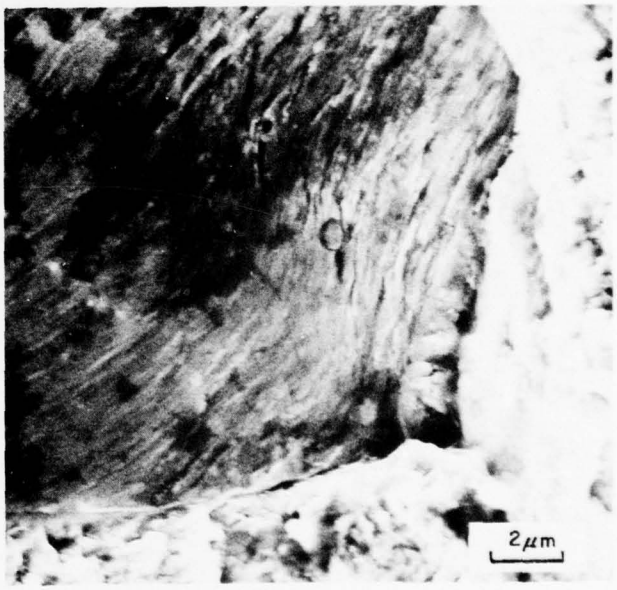

(c)
DRY NITROGEN

(d)
HUMID AIR

FE-0.05 C FRACTURE SURFACES SHOWING THE EFFECT OF CHANGE OF ENVIRONMENT.

FIGURE 6

the material. We believe that hydrogen 1) increases the flow stress of the material, i.e., makes dislocation motion more difficult, and 2) decreases the strain to fracture (ductility) of the material.

Evidence for an increase in flow stress comes from Karpenko, Yarmchenko and Shved[14] who found that thin iron specimens deformed while being charged exhibited increased flow stress and decreased elongation, while thick specimens showed no change in flow stress. The maximum change in flow stress found was 13%. Supporting evidence for hydrogen increasing the flow stress has recently been published.[20]

The changes we have found in inner cyclic plastic zone size, for the moist environment, Table I (for ΔK = 10 MN/$m^{3/2}$) may be explained by assuming an increased flow stress of 17%, which matches relatively well with that found by Karpenko, et al.[14]

The presence of the brittle-striated grains implies a localized loss in cyclic ductility caused by the influence of moisture, in agreement with the cyclic zone subcell modification already discussed. By considering the fatigue crack growth rate-ΔK dependency established in this and other studies, it is possible to derive a reasonable idea as to the cause of the embrittlement.

In Figure 7, fatigue crack growth data for mild steel, as determined by a number of researchers,[1-4, 15-19] are summarized in Table II. The Yokobori[15] steel was identical to that used in the present tests. Test environments include air (of various unknown relative humidities), dry nitrogen, and vacuum. The data generally conform to the Paris law,

$$\frac{da}{dn} \propto \Delta K^m.$$

For most of the air environments, good agreement is obtained for m ranging from 3.3 to 3.9. The only value outside of this spread is that found by Nelson,[4] m = 2.8, which also agreed with his vacuum tests. It is interesting to note that Nelson found the fracture surfaces in both his air and vacuum tests to be transgranular, and totally "ductile" in appearance, while in the

Table II. Properties of Mild Steels for which Data Is Plotted in Figure 7.

Reference	σ_y (MN m^{-2})	σ_{ULT} (MN m^{-2})	Carbon Content (%)	Elongation (%)
Priddle [16]	303	454	.23	34
Frost, et al [17]	207	289	.05	38
Yokobori, et al[3] & Present Study	218	282	.05	56
Nelson [5]	210	380	.20	30

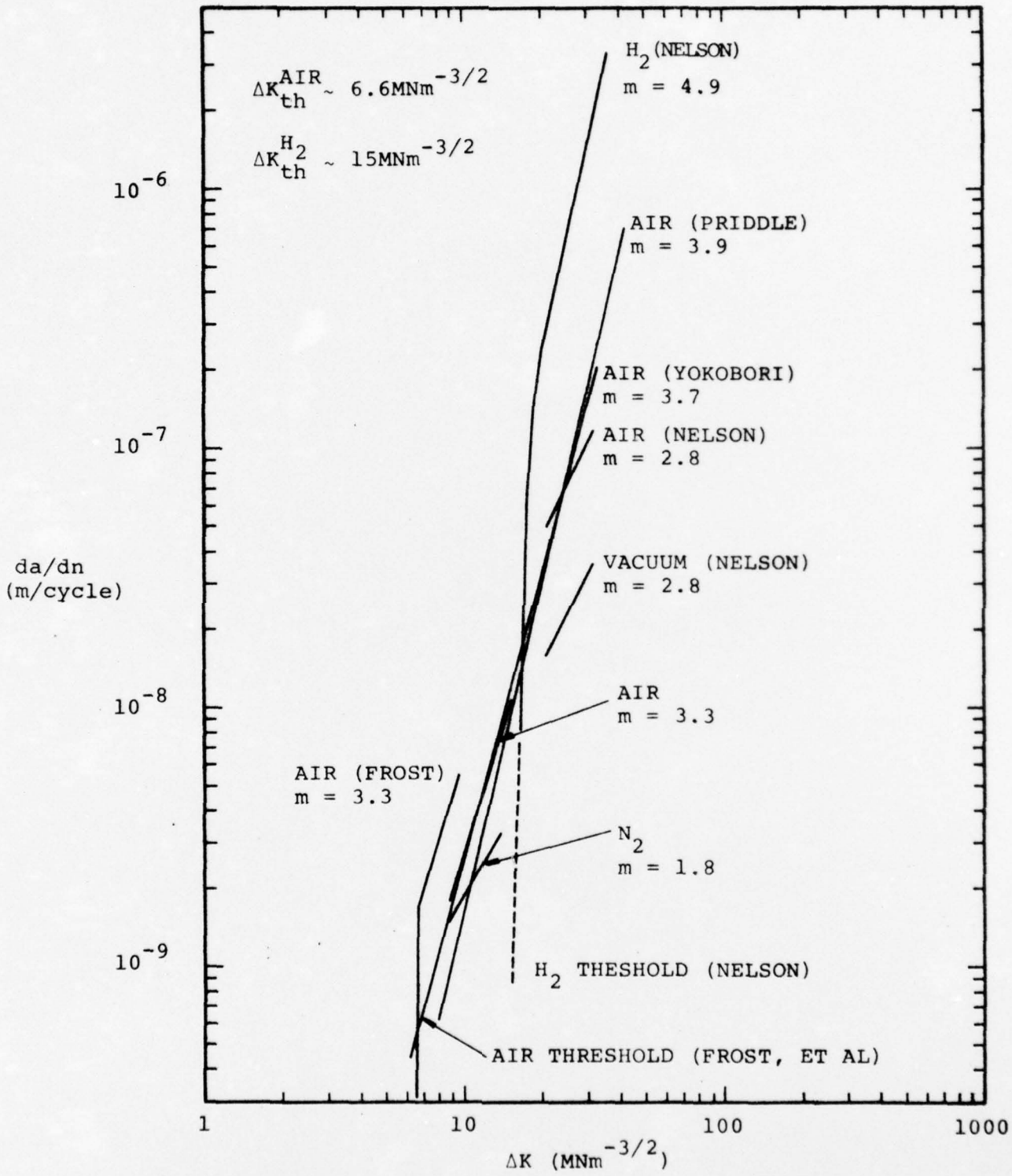

FIGURE 3. Crack Growth Rate Versus Stress Intensity for Mild Steel in Various Environments

hydrogen environment, where m was 4.9, fracture also was transgranular, but in this case it was associated with very little deformation. In fact, the fracture consisted entirely of brittle-appearing, grain-size, striated facets, similar in appearance to those encountered amongst normal ductile-striated grains in the present air environment.

Our observation of brittle facets is supported by similar findings by Kawasaki, et al.,[18] who studied a ferritic-pearlitic mild steel. It was found that interspersed among ductile striations were facet-like, transgranular regions where brittle-like fracture had occurred (study of their micrographs also seems to indicate the presence of brittle striations). In addition, investigation of fatigue crack growth in air and vacuum for high strength aluminum has shown that the higher crack growth rate for air correlates with observation of pseudo-cleavage, transgranular features on characteristic crystallographic planes.

Taken together, the above observations can be interpreted as follows. Considering that a total hydrogen environment produces a fracture surface composed of brittle-faceted striations, it is likely that it is the hydrogen in the water vapor which is responsible for the combined ductile-brittle striated fracture regions during the present air tests, as well as in others.[18] Since the air results of Nelson[4] did not show the brittle features, it is suggested that possibly the relative humidity of his air environment was sufficiently low that the hydrogen present was below the threshold necessary to cause "brittle" crack growth, hence the agreement between the crack growth law exponents (m = 2.8) for both air and vacuum.

The idea that hydrogen in the water vapor is the active atomic specie is reinforced by the observation (present work and ref.18) that the brittle-striated facets are more populous within the specimen interior. Within this nominally plane strain region, the stress state at the crack tip is known to be more triaxial than near the surface, where a more nearly plane stress situation prevails. Since hydrogen tends to congregate at hydrostatically stressed sites within crystal lattices, it is then reasonable that brittle facets, if due to the influence of hydrogen, would tend to be most prevalent at interior locations, in agreement with our observations.

The divergence of the present air and dry nitrogen data occurs below the threshold for crack growth in hydrogen, indicating the stress intensity threshold for growth in the absence of significant concentrations of hydrogen is actually lower than that when the hydrogen is present. The data of Frost, et al.,[17] show that the threshold lies at approximately 6.6 MN $m^{-3/2}$, or less than half of the H_2 threshold.[5] This effect is of considerable interest; immersion of mild steels in salt water[19] produces the opposite effect, with the threshold being essentially eliminated by this aggressive environment. Any comment at this time regarding a mechanism to explain the increase in threshold stress intensity with hydrogen content would be speculation.

E. Ion Microprobe Analysis for Hydrogen

A comparison of our experimental data with that of others, as already discussed, indicates strongly that hydrogen may be the environmental specie

responsible for the effects observed. Thus, the direct observation of hydrogen would be useful corroborating evidence. Since most matter contains hydrogen, in small amounts, it appeared to be necessary to look for a decreasing hydrogen concentration with increasing distance from the crack plane. The only instrumental technique with which we are familiar which has the spacial resolution for this observation is the ion microprobe. Dr. Dale Newbury at the National Bureau of Standards probed for hydrogen on a section of one specimen with an ion microprobe. The crack was grown alternately in wet air and dry nitrogen at three values of ΔK. The probe size used was 20μm, and all values were taken 40 μm from the crack plane. Results are shown in Table III.

Table III.

(A)

Measurement at 40μm from plane of crack.

ΔK ($MN/m^{3/2}$)	Envn.	H/Fe^{56} (10^{-3})
11	Wet	1.03
11	Dry	1.28
13.2	Wet	1.97
13.2	Dry	1.56
15.4	Wet	2.05
15.4	Dry	2.03
15.4	Dry(40μm)*	1.88
15.4	Dry(3500μm)*	1.27

*Distance ahead of crack tip

(B)

For ΔK = 13.2 $MN/m^{3/2}$, wet air

Distance ⊥ to Crack Plane(μm)	H/Fe^{56} (10^{-3})
0	1.32
25	1.49
50	1.52
72	1.61
100	1.51
200	1.50
300	1.33
500	1.36
4000	1.24

These results are intriguing, but inconclusive. There appears to be a general, small, increased hydrogen concentration with ΔK. Likewise, there appears to be maximum (27% increase)in hydrogen concentration at 72 μm perpendicular to the crack plane.

In an attempt to determine if these small increases in hydrogen were real, a small piece of the same material was half immersed in a 26% aqueous solution of sulfuric acid and hydrogen charged for 5 minutes at 0.1 amp/cm^2. This is the same technique Karpenko, et al[14] used to charge iron specimens which showed an increase in yield stress due to hydrogen. Ion microprobe analysis of the charged and uncharged specimen surfaces showed no difference in hydrogen, which is not surprising in light of the recent results reported by Lunarska[20] which indicate that hydrogen rapidly escapes undeformed iron.

The fatigue crack specimen on which the ion microprobe analysis was

performed was stored for about 2 months at room temperature between growth of the fatigue crack and the microprobe work. Hydrogen can diffuse in iron 2 cm/hr at room temperature if not locked in someway, and it is unknown whether or not the binding energy between dislocations and hydrogen is sufficient to lock the hydrogen. Thus, it is not known whether it is even feasible to search for hydrogen in this type of experiment.

F. References

1) D. L. Davidson and J. Lankford, ONR Interim Report, 6 August 1976.

2) D. L. Davidson and J. Lankford, Fracture 1977, Volume 2 University of Waterloo Press, Waterloo, Ontario, Canada, p. 897-904.

3) T. Yokobori, K. Sato, and Y. Yamaguchi, Reports of the Research Institute for Strength and Fracture of Materials Vol. 6 (2) 49 (1970).

4) H. G. Nelson, Proceedings Second International Conference on Mechanical Behavior of Materials, ASM 1976, p. 690-4.

5) H. G. Nelson, The Effect of Hydrogen on Behavior of Materials, ed. A. W. Thompson and I. M. Bernstein AIME 1975, P. 602-10.

6) F. V. Lawrence and R. C. Jones, Met. Trans. 1 367-376 (1970).

7) H. Mughrabi, K. Herz and X. Stark Acta. Met. 24 659-668 (1976).

8) S. Ikeda, Y. Izumi, and M. E. Fine, Engineering Fracture Mechanics 9 123-136 (1977).

9) M. E. Fine and Y. Izumi, "Fourth International Conference on the Strength of Metals and Alloys" private transmittal of preprint, Jan. 1977.

10) Y. Izumi, private communication, Jan. 1977.

11) J. Petit, B. Bouchet, C. Gase, and J. de Fouguet, Fracture 1977 2, University of Waterloo Press, 1977, p. 867-872.

12) E. F. Smith III, R. J. Jack, and D. J. Duquette Deuxieme Congres International L'Hydrogene dans les Metaux 1977, paper 3C1 (preprint)

13) H. L. Marcus, Proceedings of the Environmental Degradation of Engineering Materials Conference, VPI, Blacksburg, VA, Oct. 12-19, 1977 (preprint).

14) G. V. Karpenko, N. Ya Yarmchenko, M. M. Shved, Soviet Materials Science 7(3) 304-306 (1971), Translation Oct. 1973.

15) T. Yokobori, K. Sato, and Y. Yamaguchi, "X-ray Microbeam Studies on Plastic Zone at the Tip of the Fatigue Crack," Rep. Res. Inst. Strength and Fracture Mat., Vol. 6, 1970, 49.

16) E. K. Priddle, "High Cycle Fatigue Crack Propagation Under Random and Constant Amplitude Loading" Int. J. Press. Ves. and Piping, Vol. 4, 1976, 89.

17) N. E. Frost, L. P. Pook, and K. Denton, Eng. Frac. Mech., Vol. 3, 1971, 109.

18) T. Kawasaki, T. Yokobori, and S. Nakanishi, "Fractographical Study on Fatigue Crack Propagation in a Structural Carbon Steel by Scanning Electron Microscopy," Rep. Res. Inst. Strength and Fracture Mat., Vol. 6, 1970, 1.

19) W. Elber, Eng. Frac. Mech., Vol. 2, 1970, 37.

20) E. Lunarska, Scripta Met. 11(4) 283-288 (1977).

II. THE USE OF ELECTRON CHANNELING IN THE STUDY OF MATERIAL DEFORMATION

The following article appeared in Scanning Electron Microscopy/1977 Vol. I from the proceedings of the Workshop on Analytical Electron Microscopy, IIT Research Institute, Chicago, Illinois. (March, 1977)

SCANNING ELECTRON MICROSCOPY/1977 Vol. I
Proceedings of the Workshop on
Analytical Electron Microscopy
IIT Research Institute
Chicago, Illinois 60616, U.S.A.
March 1977

THE USE OF CHANNELING CONTRAST IN THE STUDY OF MATERIAL DEFORMATION

David L. Davidson
Southwest Research Institute
P. O. Drawer 28510
San Antonio, Texas 78284

Abstract

Channeling contrast is one way the mechanism of electron channeling may be used in deformation studies. This technique is in many ways complementary to the study of deformation using selected area electron channeling patterns, in that it allows subgrain formation and refinement to be followed during the deformation process. Electron channeling patterns are the most useful, conversely, in defining the initial stages of deformation. Together, the two techniques can be powerful tools in the study of dislocation substructural development in bulk materials. Channeling contrast occurs because of differences in the scattering of the incident electron beam by different crystallographic orientations of adjacent regions of the crystallites being observed. Channeling contrast is observable in a standard SEM with no modification. A convergent beam is used to obtain the desired resolution, although it is important to minimize beam divergence. The width of a channeling line determines the grain size which will exhibit uniform contrast. Maximum benefit of the channeling contrast technique may be obtained when used together with selected area channeling patterns. The complementary use of channeling patterns and channeling contrast is illustrated for 304 stainless steel fatigue specimens observed prior to crack initiation. Subgrain formation adjacent to fatigue cracks in low carbon steel and an aluminum alloy are used to illustrate the advantages and limitations of the channeling contrast technique.

Key Words: Electron Channeling Contrast, Microstructure, Subgrain Formation, Selected Area Electron Channeling Patterns, Fatigue, Fatigue Crack Propagation, Scanning Electron Microscopy

Introduction

Information related to the crystallographic orientation and defect structure of crystalline materials may be gained by using the SEM in the electron channeling mode. The electron channeling phenomena may be exploited in three ways: (I) channeling patterns superimposed on a secondary electron image,[1] (II) selected area electron channeling patterns,[2] and (III) crystallographic contrast, also called channeling contrast,* diffraction contrast, and grain contrast.[3] Good review articles exist on nearly all aspects of channeling.[4,5,6]

The most exploited of the channeling techniques has been electron channeling patterns. The reviews[4,5,6] give excellent examples of their use for both crystallographic and deformation studies. Channeling contrast, conversely, has not been extensively exploited, although there are several papers covering various aspects of the technique.[7,8,9]

Selected area electron channeling patterns contain information directly related to the crystallographic structure and orientation of the volume interrogated by the beam. Channeling pattern line acuity and contrast changes known to be due to the introduction of defects into the crystal may be used as an indirect method of assessing the magnitude of damage to the crystal. Channeling contrast, although originating from spatial crystallographic differences in the material, can be used for crystallographic orientation only in rare instances. But it can be used for the direct assessment of crystallite deformation because of the propensity of dislocations in many materials to form into networks. In many ways, channeling contrast provides complementary information to that provided by channeling patterns. The purpose of this paper is to

*The author prefers this term because it relates the contrast observed to the physical phenomena of electron channeling from which it originates.

indicate the broad range of usefulness of the channeling contrast technique to materials research, to bring together some of the scattered information on the subject, and to further discuss and elucidate some of the experimental factors to be considered when using the technique. The complementary uses of channeling contrast and channeling patterns will be emphasized.

Origin of Channeling Contrast

The origin of channeling contrast is the same as that of channeling patterns. The impinging beam is scattered as the electrons encounter individual planes of atoms within the crystal. The magnitude of the scattering depends upon the relative angle between the beam and the atomic planes and upon the (Rutherford) scattering mechanism. The physics of channeling has been described[4,9] and thoroughly explored (see the bibliographic compilation on channeling in these proceedings). Changing the angle of the beam, through scanning, changes the magnitude of the scattering. Thus, there is a relationship between the crystallographic orientation of a grain and the angle of the impinging beam which causes different grains to exhibit different gray levels. Changes in crystallographic orientation as small as 0.1 degrees may be observed. It is the ability to detect such small changes which makes channeling contrast useful.

Obtaining Channeling Contrast

Channeling contrast may, in theory, be obtained with any commercially available SEM; all that is necessary is that the instrument be capable of detecting either backscattered electrons or absorbed electrons (specimen current imaging). In practice, having a backscattered detector coaxial to the incoming beam increases resolution of the backscattered images by increasing the proportion of collected backscattered electrons,[10] thus allowing the use of decreased beam currents. Specimen current imaging theoretically should give the same resolution as backscattered electrons imaging, but in practice, characteristics of the specimen current amplifier are a limiting factor (for a complete discussion of this subject, see Newbury[11]).

Optimum electron optical conditions necessary to obtain channeling contrast depend on the specimen being observed as well as the design and construction of the SEM. Typical operating conditions[7] are a beam divergence of 2-4 X 10^{-3} rad, accelerating voltages of 10-30 kV, specimen currents of about 5 X 10^{-9} amps for aluminum and 2 X 10^{-9} amps for iron. Assuming proper surface preparation, obtaining useful micrographs is dependent on developing sufficient channeling contrast. To obtain contrast, a sufficient number of incident electrons must be backscattered from the specimen to allow a detectable signal above the noise[12] to be recorded. Since the number of incident electrons which are backscattered is atomic number dependent,[13] development of contrast in materials of differing atomic number requires different beam current. Thus, for a given material, beam current, as observed by specimen current, and frame time for the micrograph are the important parameters. It may be desirable with some materials which oxidize readily, such as aluminum alloys, to use 30 kV together with higher beam current and sacrifice resolution in order to minimize the effect of the oxide layer. With a tungsten hairpin filament, the probe diameters common for channeling contrast are about[8] 0.4 μm for iron and 0.7 μm for aluminum alloys (calculated values[12,13]).

Careful materials preparation is vital. Final surface preparation by chemical or electropolishing is typically required for metals, although electrolytic lapping has also been used successfully. See the Appendix for details.

Use of Channeling Contrast in Deformation Studies

Although it is almost as easy to make channeling contrast micrographs in the SEM as it is to make secondary electron micrographs, there are a number of experimental factors which must be considered in applying the technique to study deformation. Some aspects of the use of channeling contrast have been briefly discussed by several authors.[8,9,14] Their discussion, together with further experimentation, indicates that it is useful to consider grain size as either "large" or "small," depending upon the size of the grains relative to the width of the channeling bands. These are dependent upon the crystal structure and interplanar spacing of the material, the accelerating voltage, and magnification (scan angle). "Large" grains, which must be examined at low magnification (relatively large scan angles), may exhibit channeling bands within the grain,[9] Figure 1. This contrast is unrelated to deformation. The grain size and magnification combination giving grains of a uniform gray level depends on the orientation of the grain. The gray level of any grain is dependent upon the gray level at the center of a channeling pattern of that grain. If the center of the pattern is on one edge of a channeling band (a channeling line), then the width of that channeling line, relative to the grain size, will determine the contrast within the grain, the grain being of uniform contrast if it is smaller than the line width. Channeling line width, 2 w_g, is dependent upon accelerating voltage, atomic number, and grain orientation. From Schulson[15]

$$w_g = \frac{1}{\xi_g |g|} \qquad (1)$$

where ξ_g = extinction distance,[16] and $|g|$ = reciprocal lattice vector magnitude. Table I gives calculated values of w_g for aluminum and iron.

TABLE 1. CALCULATED VALUES IN RADIANS/DEGREES OF w_g FROM EQUATION (1)

Material	Planes	w_g (20 kV)	w_g (30 kV)
		X 10^{-3} rad/degrees	
Fe	200	3.37/0.193°	2.79/0.160°
	222	2.03/0.116°	1.69/0.097°
	521	0.63/0.036°	0.53/0.030°
Al	200	2.73/0.156°	2.25/0.129°
	222	1.71/0.098°	1.41/0.081°
	531	0.49/0.028°	0.41/0.023°

For high index planes, the width of the channeling line becomes very narrow; thus, they cannot be resolved with the angular divergences necessary for a focused beam. The contrast from higher order lines is also very poor; for example, the 222 and 333 lines seen in Figure 2a_1 are narrow and exhibit poor contrast. Thus, it is likely that only low index lines will be visible in the convergent beam (micrograph) mode, even when the grain size is sufficiently large, and the magnification low, to allow observation of channeling lines, as seen in Figure 1. For the (200) band in Al, only grains larger than about 60 μm could exhibit nonuniform contrast. For Fe, grain sizes of about 70 μm would be required.

In the absence of texturing, random grain orientation yields only a small number of grains with low index lines; thus, uniform gray levels will be experienced for much larger grain sizes than indicated above. It is best to determine experimentally if the grain size in the material of interest exhibits uniform grain contrast.

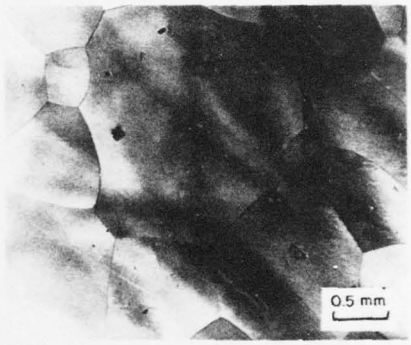

FIG. 1 - Channeling bands imposed on the grain structure of large grained, undeformed platinum. Surface preparation by electrolytic lapping.

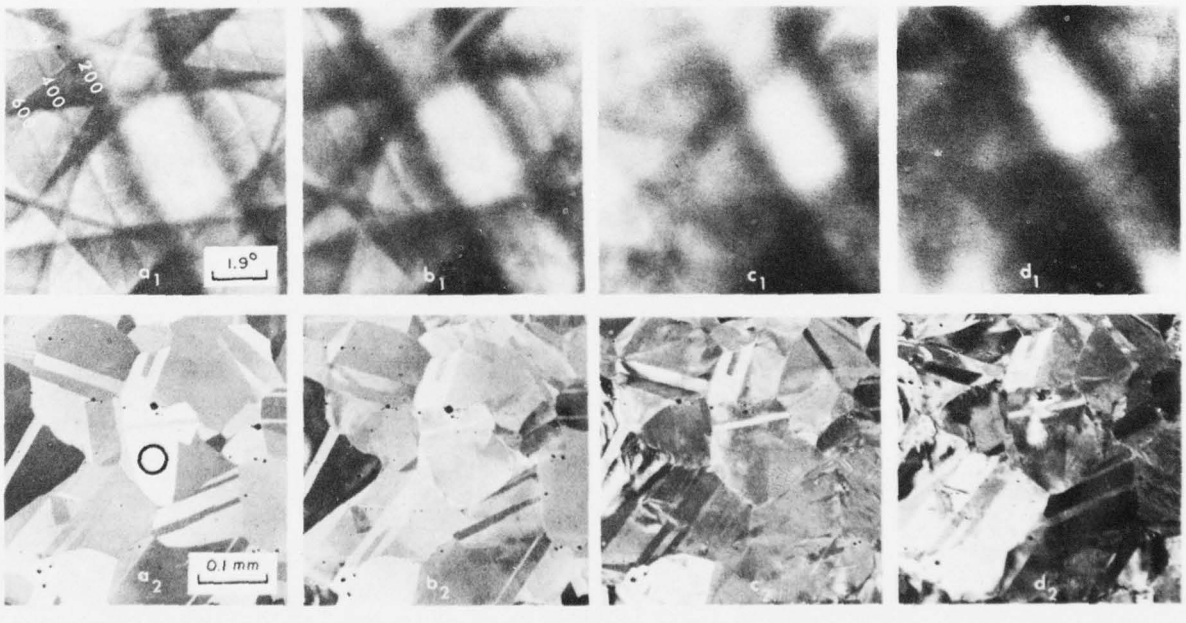

(a) (b) (c) (d)

FIG. 2 - Comparison between channeling pattern change and subgrain formation in 304 stainless steel. (a) before cycling, (b) after 4 cycles, ± 1% strain control, (c) after 32 cycles, (d) after 128 cycles. Area of channeling pattern as shown in (a) is the same for (b)-(d).

Many deformation studies by transmission electron microscopy, X-ray topography, etch pitting, and optical microscopy have shown that deformation at near ambient temperatures in polycrystalline, fully recrystallized metals proceeds in approximately the following steps:[17,18]

(1) Single slip occurs in a few grains.
(2) Multiple slip systems are activated as sufficient strain (2-3% for cubic metals) is accumulated to require accommodation shape changes between grains. Many grains are now deforming by multiple slip and have approximately equal dislocation densities, although variations from grain to grain and within single grains still exist, and in some cases will persist to large strains.
(3) Dislocations begin to accumulate into superstructures, forming boundaries within the original grains.
(4) As deformation continues, the number of subgrains increases, decreasing the average subgrain diameter, and usually increasing misorientation between adjacent subgrains.

Details of these processes depend upon the mode of deformation (monotonic, cyclic, creep, etc.), grain size, temperature, deformation rate, and perhaps environment.

Selected area electron channeling may be used to follow Steps 1 and 2. Deformation during Step 3 becomes so large that useful information is no longer available. Channeling contrast begins to be useful during Step 3, allowing subgrain refinement to be followed to submicron sizes. It is the ability of these two complementary electron channeling techniques to follow the deformation process in bulk materials that makes them such attractive tools in studying metallurgical and mechanics related engineering problems, such as creep and fatigue.

As has been shown by several investigators,[7,8,14] the gray level often changes as the specimen is translated, rotated, or tilted beneath the electron beam. Thus, it may be necessary to observe a specimen in several positions in order to develop gray level differences between adjacent subgrains. The magnitude of misorientation between subgrains dictates the necessity for making multiple micrographs of a region of interest. It has been observed experimentally that it is necessary to make multiple micrographs for small amounts of deformation, but that as deformation proceeds and subgrain misorientation increases, little information is gained from multiple micrographs. Optimization of electron-optical and photographic parameters, together with the ability of the eye to distinguish up to 20 gray levels,[19] minimizes the necessity for making multiple micrographs.

Channeling contrast effects have been illustrated for deformation in tension,[7] and in creep.[8] The technique has proven to be particularly useful in the study of fatigue, as Figures 2, 3, and 4 illustrate. Fatigue crack initiation may be related to the formation of subcells in the near surface region, and subcell formation is known to occur in the material just adjacent to a propagating fatigue crack; yet these processes are difficult to follow with conventional investigative methods. The development of subcells and changes in the channeling patterns caused by cyclic loading is illustrated in Figure 2. In this 304 stainless steel specimen, a number of areas were selected prior to cycling, with both channeling contrast micrographs and selected area channeling patterns being made, Figures $2a_1$ and $2a_2$. The specimen was then cycled under strain control ($\pm$ 1.0%) in an electrohydraulic testing machine and periodically removed for observation in the SEM.* Observation with a progressively increasing number of cycles illustrates well the complementary use of both techniques. After four cycles, Figure $2b_1$, the channeling pattern begins to lose line acuity, as may be seen particularly well by comparison of the numerous fine, higher order lines of Figures $2a_1$ and $2b_1$. These changes correspond to an equivalent tensile deformation of approximately 0.3%.[20] Little subgrain formation is visible, Figure $2b_2$. After 32 cycles, the channeling pattern, Figure $2c_1$, indicates about 2.5% strain. This deformation is occurring inhomogeneously between grains, as may be seen in Figure $2c_2$. Subgrains are not forming equally in each part of each grain. After 128 cycles, some additional change has occurred in the channeling pattern, Figure $2d_1$, which now is indicating a level of about 5% strain. The channeling micrograph, Figure $2d_2$, now indicates that extensive subgrain formation is taking place in the surrounding grains. These observations indicate that an assessment of deformation during the first few cycles is best made indirectly and on a local basis, using channeling patterns because of their sensitivity to small magnitudes of deformation. After 32 cycles, direct observation of the deformation over a larger area using channeling contrast is preferred due to the formation of dislocation subcells and because channeling patterns are much less sensitive to small increments of deformation at relatively large deformation magnitudes. Stress versus strain records for each cycle indicated no change after about 50 cycles, although the micrographs clearly indicate the continuing formation of subcells.

Fatigue crack propagation studies in a 0.05 wt.% carbon steel have allowed determination of the effects of cyclic loading parameters and environment on crack propagation through the use of channeling contrast.[21,22] Typical subgrain formation for this material is shown in Figure 3. It is not possible to obtain useful electron

*More experimental details may be found in the Appendix.

channeling patterns for this material due to the dislocation density inherent in the allotropic transformation in iron-carbon alloys. From micrographs such as these, subgrain size as a function of distance from the crack plane has been determined to be a function of both loading magnitude and environment. It was found that tilting or translating the specimen for making multiple micrographs was unnecessary, presumably because of the large subgrain misorientation. Subgrain sizes of 0.5-1 μm are readily observed using the electron optical conditions given in the second paragraph of the third section of this paper. Thus, the actual probe sizes appear to be somewhat smaller than those calculated.

Fatigue crack plasticity studies in aluminum alloys[23,24] have indicated that the plasticity information is available from the channeling patterns rather than from channeling contrast. Occasionally subgrains can be brought out in these alloys if just the correct combination of electron optical conditions and grain orientation occurs. The crack tip region depicted in Figure 4 shows the apparent formation of a few large subgrains to the left of the crack. Note that the contrast changes from light on the right to dark on the left, with the reversal being at just about the crack plane. A channeling pattern of the grain shows it to be oriented at the edge of the ⟨200⟩ band so that the contrast reversal is due to one line of that band. Thus, the ability to detect subgrains in this situation is dependent upon obtaining the proper grain orientation, relative to the probe, so that small contrast changes can be detected. Depending on grain orientation, specimen reorientation beneath the beam, together with multiple micrographs, may prove to be very useful. To obtain channeling contrast in the aluminum alloys, fairly large beam currents are required (a limitation of source brightness), causing probe sizes in excess of 1 μm (see earlier discussion). Transmission electron microscopy studies have shown[25] that subgrain formation in these alloys usually occurs very near the crack plane, and that most subgrains are in the size range 0.1 to 1 μm. Thus, the electron-optical-material conditions will allow only the revelation of the few larger subgrains present. Depending on the crystallographic orientation of the grain to the stress field of the crack, subgrains of detectable sizes may or may not be formed.

Conclusion

Electron channeling contrast is an important tool for the materials scientist, particularly in studies of crystalline solids where the formation of subcells is an important factor. Subgrain formation may, for the first time, be followed in bulk, technologically useful alloys, where repetitive observation of the same grains is possible as the substructure develops. Fortunately, any standard SEM may be used for channeling contrast observations. No modifications, such as those necessary for obtaining selected area electron channeling patterns, are necessary for this mode of observation. Although cyclic loading is emphasized in the illustrations, monotonic loading, time dependent and environmentally sensitive deformation may be observed as well. In using the channeling contrast technique, however, it is necessary to be aware of the electron optical and crystallographic circumstances which allow observation of the effects desired. For optimum use of the technique, coordinated use of channeling patterns is also desirable, since the two techniques are largely complementary.

References

1. D. G. Coates, "Kikuchi-like Reflection Patterns Obtained with the Scanning Electron Microscope," Phil. Mag. 16 1967, 1179-1184.

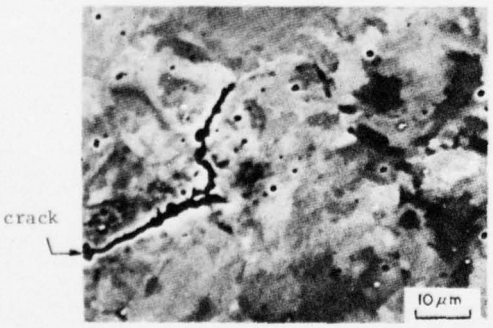

FIG. 3 - Subgrain formation by fatigue crack passage in Fe-0.05 C alloy. Subgrain formation has completely obscured the normal grain structure (23 μm). ΔK = 26 MN/m$^{3/2}$.

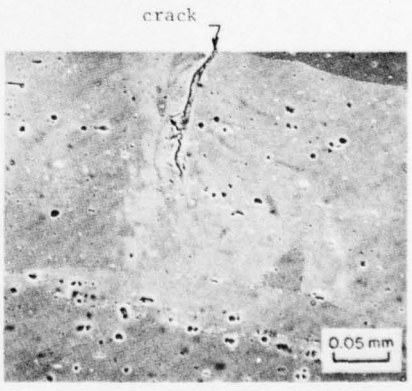

FIG. 4 - Subgrain formation by fatigue crack passage in 6061-T6 aluminum alloy. Subgrains are visible because of a favorable grain orientation relative to the crack and to the probe. ΔK = 10.4 MN/m$^{3/2}$.

2. E. M. Schulson and C. G. van Essen, "Optimum conditions for generating channeling patterns in the scanning electron microscope," J. Phys. E. 2 1969, 247-251.
3. G. R. Booker, "Electron Channelling Effects Using the SEM," IITRI/SEM/1970, 489-496.
4. G. R. Booker, "Scanning Electron Microscopy. Electron Channelling Effects," in Modern Diffraction and Imaging Techniques in Materials Science, S. Amelinckx, R. Gevers, and G. Renaut (Eds.), American Elsevier, New York, 1970, pp. 613-652.
5. D. C. Joy, "Electron Channelling Patterns in the SEM," in Quantitative Scanning Microscopy, D. B. Holt (Ed.), Academic Press, London, 1974, pp. 131-182.
6. D. C. Joy, "The observation of crystalline materials in the scanning electron microscope (SEM)," J. Microscopy 103 1975, 1-23.
7. D. C. Joy, D. E. Newbury, and P. M. Hazzledine, "Anomolous Crystallographic Contrast on Rolled and Annealed Specimens," IITRI/SEM/1972, 97-104.
8. D. C. Joy and G. R. Booker, "Recent Developments in Electron Channelling Techniques," IITRI/SEM/1973, 137-144.
9. D. E. Newbury, "The Origin, Detection, and Uses of Electron Channelling Contrast," IITRI/SEM/1974, 1047-1057.
10. E. D. Wolf and T. E. Everhart, "Annular Diode Detector for High Angular Resolution Pseudo-Kikuchi Patterns," IITRI/SEM/1969, 41-44.
11. D. E. Newbury, "The Utility of Specimen Current Imaging in the SEM," IITRI/SEM/1976/I, III. 120.
12. D. C. Joy, "The Scanning Electron Microscope—Principles and Application," IITRI/SEM/1973, 743-750.
13. C. W. Oatley, The Scanning Electron Microscope, Part 1. The Instrument, Cambridge Univ. Press, London, 1972, p. 149.
14. M. Pitaval, G. Blanchin, E. Vicario, and G. Fontaine, "Crystalline Contrast and S.E.M. Channeling Patterns," Proc. 25th Anniv. Meeting of Electron Micro. and Analysis Group, Institute of Physics, London, 1971, pp. 338-340.
15. E. M. Schulson, "Interpretation of the Widths of SEM Electron Channelling Lines," phys. stat. sol.(b) 46 1971, 95-101.
16. P. B. Hirsch, A. Howie, R. B. Nicholson, D. W. Pashley, and M. J. Whelan, Electron Microscopy of Thin Crystals, Butterworths, London, 1965, Appendix 4, pp. 495-497.
17. D. McLean, Mechanical Properties of Metals, Wiley, New York, 1962, p. 122.
18. W. A. Backofen, "Deformation Processing," Met. Trans. 4 1973, 2679-2699.
19. D. E. Newbury, "Techniques of Signal Processing in the Scanning Electron Microscope," IITRI/SEM/1975, 727-736.
20. D. L. Davidson, "A Method for Quantifying Electron Channeling Pattern Degradation Due to Material Deformation," IITRI/SEM/1974, 927-934.
21. D. L. Davidson, J. Lankford, T. Yokobori, and K. Sato, "Fatigue crack tip plastic zones in low carbon steel," Int. J. Fracture 12 1976, 579-585.
22. J. Lankford and D. L. Davidson, "Environmental Alteration of Crack Tip Dislocation Cell Structure and Mode of Growth During Fatigue Crack Propagation in Ferritic Steel," Int. J. Fracture 12 1976, 575-576.
23. D. L. Davidson and J. Lankford, "Plastic Strain Distribution at the Tips of Propagating Fatigue Cracks," J. Engg. Matls. and Technol. (ASME) 98 Series H 1976, 24-29.
24. J. Lankford and D. L. Davidson, "Fatigue Crack Tip Plasticity Associated with Overloads and Subsequent Cycling," J. Engg. Matls. and Technol. (ASME) 98 Series H 1976, 17-23.
25. J. C. Grosskreutz and G. G. Shaw, "Microstructures at the Tips of Growing Fatigue Cracks in Aluminum Alloys," Fatigue Crack Propagation, ASTM STP-415, Amer. Soc. Test. Mat., Philadelphia, 1967, 226-243.

Acknowledgment

Financial support for portions of the work reported here has come from the Office of Naval Research through Contract N00014-75-C-1038.

Appendix (Experimental Details)

The ETEC, Inc., SEM used in these experiments was fitted with an after lens deflection coil for making selected area electron channeling patterns. Channeling contrast was detected with a solid state silicon solar cell detector mounted beneath the after lens coil. A working distance of 25 mm and a 100 μm objective aperture were used, with a zero specimen tilt. Observations were made using either 20 or 30 kV.

Cyclic loading of the 304 and 6061 specimens was done external to the SEM. Periodically, the cyclic experiments were interrupted and the specimens examined in the SEM. The low carbon steel specimens were cut from the center of a large center-notched fatigue specimen at termination of a test program, metallurgically mounted and ground, using typical metallographic methods, and then electropolished.

Prior to deforming any specimen which is to be examined by the channeling mechanism, careful heat treatment and surface preparation are normally necessary. The heat treatments used were: solution treatment, quenching and aging for the aluminum alloy,[23] solution treatment and furnace cool for the stainless steel,[20] and furnace anneal for the low carbon steel.[21] Standard electropolishing techniques[16] were used as the final step in preparation for all specimens except the platinum, which used a Struers electrolytic lapping process. Occasionally, an intermediate electropolish is necessary during a long series of experiments requiring interspersed cyclic loading and SEM examination. The necessity for repolishing is evidenced by observable surface contamination.

Discussion with Reviewers

Reviewer III: In reference to the line width the author is requested to comment on the effects of beam divergence and crystalline perfection of the specimen on the observed contrast effects (G. R. Booker and R. Stickler, 5th Interm. Materials Symp., Univ. of Cal., Berkeley 1971, Univ. Press, 1972).

Author: The reference given by the reviewer is one of several which emphasizes the necessity to establish a beam divergence less than that of the higher order lines to be observed. The reader is also encouraged to become familiar with the Appendix to text reference 15, which has a good discussion of this point. In deformation studies, it is very helpful to heat treat specimens so as to minimize initial dislocation density (giving high crystalline perfection). This is desirable in order to maximize the sensitivity of the technique for observing changes in crystalline perfection, and so that interpretation of channeling pattern changes will be as unambiguous as possible.

Reviewer III: Would the author indicate the amount of strain he deduces from the SACPs in Fig. 2 and the method he used to obtain this quantitative information?

Author: The amount of strain in Figure 2, as given in the accompanying text on the page following Figure 2, was deduced using the comparison technique fully explained in text reference 20.

Reviewer III: Depending on grain orientation how many channeling contrast micrographs are required to reveal positively all subgrains present?

Author: Although this point was mentioned in the text, it should be said again that the number of micrographs must be assessed experimentally for the material of interest. For the low-carbon steel, it was found to be of greater advantage to "serially section" the grains by short periods of electropolishing, followed by examination, than it was to make multiple micrographs of one section. In this way, an assessment of subgrain extent and shape may also be made. An example of this is included in Figure R-1. I would like to emphasize again that my observations are that multiple micrographs are more necessary for small magnitudes of deformation in relatively large grained material.

Reviewer II: Since channeling contrast originates very near the surface, how faithfully do you feel your results of substructure near a crack tip represent the substructure in the bulk? Can the proximity of the surface alter this structure?

Author: Our experience is that the substructure near a crack tip in the metals we are examining is altered very little, if any at all, by the proximity of the surface, except in the sense of fracture mechanics, which indicates that it is difficult to maintain plane strain conditions near a surface (which removes the material constraints necessary for plane strain). For fatigue cracks, we find that for very low cyclic stress intensities, there is no difference between observations made at the surface and those made from deep sections. See: D. L. Davidson, "Fatigue Crack Tip Plastic Zone Size and Shape Through the Specimen Thickness," Int. J. Fracture 11 1975, 1047-1048. Creation of a surface in very soft single crystals might allow dislocations to "leak out" prior to observation, but for the engineering materials we have examined, our assessment is that the probability of this occurring is small.

Note: The author is indebted to Reviewer II for pointing out that the publication, "Observations on the Practical Applications of Selected Area Electron Channelling Patterns to Deformation Studies," by J. A. Cornie, D. L. Harrod and C. W. Hughes, Westinghouse Research Laboratories Scientific Paper 73-ID4-HTRFC-P1, June 7, 1973, has now been published (see No. 25* of the Channeling Bibliography). The section of this work entitled "Channelling Microscopy" indicates that subcell formation is not much different when the specimen is deformed in tension or compression.

Reviewer I: Since many microscopes are operated with the specimen highly tilted, typically 45°, to produce optimum emissive mode images, is there any effect on channeling contrast images of grains from the development of asymmetry in the channeling line profiles from a tilted crystal, i.e., the lines become either white or black instead of a black/white close pair?

Author: Although I have performed no experiments to confirm it, there would be little or no effect on the channeling contrast expected from having a tilted specimen. Line contrast reversal would be expected to occur only in the higher order lines (see text reference 4, pp. 649-652), which should exert little influence on the contrast developed within a grain.

Reviewer II: What is the origin of the contrast reversal between some of the grains and twins seen in Figure 2 when going from the annealed to the strained condition?

Author: Since contrast is determined by the gray level of the center of the channeling pattern for a particular grain, the position of the specimen relative to the beam is very important. Periodic movement of the specimen from the SEM to the testing machine caused slight changes in the relative position of the specimen and the electron beam, and this is the origin of the contrast changes seen in Figure 2. Tilting the specimen could have given the same effect.

Reviewer II: What is the nature of the fine (dendrite-like) structure which appears in strong contrast in Figure $2c_2$, faintly in $2d_2$ and is absent in $2a_2$ and $2b_2$?

*See pages 445-454, these proceedings.

Author: The dendritic structure is an artifact which occurred during electropolishing. As mentioned in the Appendix, it is necessary to be very careful to prevent contamination of the surface being observed, and should such contamination occur, then reelectropolishing is required. Sometimes artifacts, such as the dendritic looking one on $2c_2$, appear. So far, their presence has not indicated any general surface contamination. The same artifact does not appear in Figure $2d_2$ because a very short electropolish was employed after 128 cycles, prior to observation. Very little metal was removed by these interim polishing operations, as a close examination of Figure 2 will show, and a clean surface for observation was ensured.

Reviewer IV: Can the misorientations between subgrains for a specimen such as that of Fig. 2d be determined from the corresponding channeling contrast micrograph?
Author: No orientation usually cannot be determined from channeling contrast micrographs.

Reviewer IV: What are the arguments for supposing that the optimum electron accelerating voltage for channeling contrast is 10 to 30 KV?
Author: Best contrast as related to signal-to-noise ratio has been determined to be developed in this voltage range. Lower voltage causes problems with oxide penetration also. Higher voltages cause decreased contrast which may be overcome with higher brightness sources. See J. P. Spencer, C. J. Humphreys and P. B. Hirsch, "A Dynamical Theory for the Contrast of Perfect and Imperfect Crystals in the Scanning Electron Microscope using Backscattered Electrons." Phil. Mag. 26, 1972, 193-213.

Reviewer IV: Is the progressive deterioration in channeling pattern quality shown in Figs. 2a to d due mainly to plastic strains (dislocations) or elastic strains?
Author: It has been shown that changes in channeling patterns are caused by dislocations rather than elastic strains. See text Reference 8, p. 140.

Reviewer IV: If satisfactory channeling patterns could be obtained from specimen areas as small as 0.1 μm across, would this be helpful for metallurgists investigating deformation problems?
Author: Yes, misorientation between subgrains is of interest to metallurgist because it is related to deformation magnitude, temperature, perhaps strain rate, metallurgical structure, and environment.

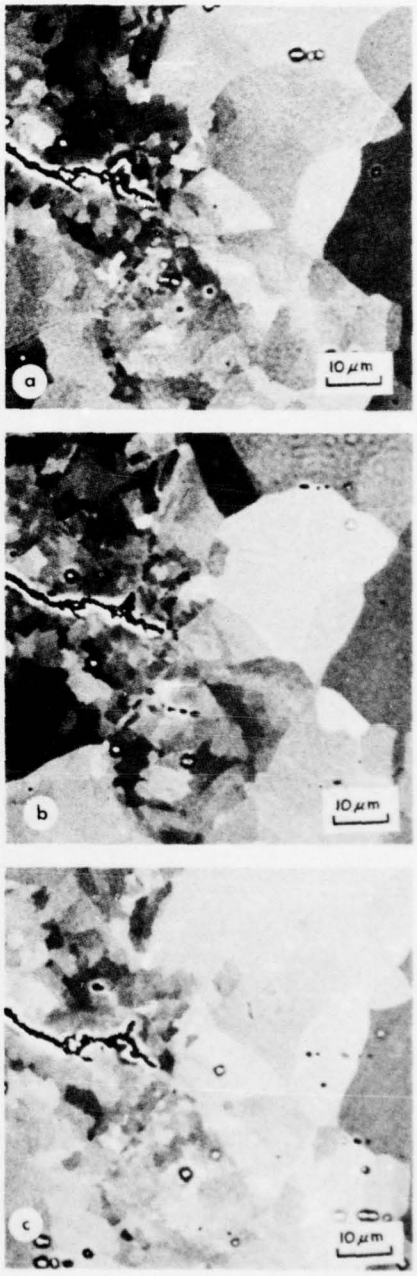

FIG. R-1 - Sectioning of grains around the tip of a fatigue crack in Fe-0.05 C, showing the change in subcell arrangement with progression through the grain structure. (Figures b and c were taken after 2 and 4 minutes additional time of electropolishing at 22v in 133 ml acetic anhydride, 7 ml water and 20 gms chromic acid, at 18 C.)